Journal of Nuclear Materials 465 (2015) 28–33

Contents lists available at ScienceDirect

Journal of Nuclear Materials

journal homepage: www.elsevier.com/locate/jnucmat

A thermo-gravimetric analysis study on the chlorination reaction of ZIRLO cladding hulls

Min Ku Jeon [a, b, *], Yong Taek Choi [a], Jin-Mok Hur [a], Do-Hee Ahn [a, b]

[a] Nuclear Fuel Cycle Process Development Division, Korea Atomic Energy Research Institute, Daedeok-daero 989-111, Yuseong-gu, Daejeon 305-353, Republic of Korea
[b] Department of Quantum Energy Chemical Engineering, University of Science and Technology, Gajeong-ro 217, Yuseong-gu, Daejeon 305-350, Republic of Korea

ARTICLE INFO

Article history:
Received 13 March 2015
Received in revised form
18 May 2015
Accepted 24 May 2015
Available online 3 June 2015

Keywords:
ZIRLO
Chlorination
Thermo-gravimetric analysis
Cladding hull waste
Reaction model

ABSTRACT

A thermo-gravimetric analysis system for hull chlorination reaction (TGA-HC) was employed to measure weight change of ZIRLO cladding hulls in-situ during the chlorination reaction. The total flow rate (Q) experiments suggested that the chlorination reaction of ZIRLO is within the gas phase transport limited region for Q of 120 and 240 mL/min conditions. The Sharp–Hancock plot was employed to determine the most suitable geometry function, and the volumetric contraction model was identified as the best model although it is valid only in a reaction progress range of (0–0.5). The effect of chlorine partial pressure (pCl_2) on the reaction rate was investigated for pCl_2 of 9.21, 16.9, and 23.4 kPa, and it was identified that the chlorination rate is proportional to chlorine partial pressure on the order of (0.873). An activation energy of 7.21 kJ/mol was achieved from reaction temperature experiments, but the value was not decisive because increasing reaction temperature also affected the gas phase transport rate. Thus, the final reaction equation rate was achieved as a function chlorine partial pressure as follows:

$$\frac{d\alpha}{dt} = 3 \times (0.00738 \times pCl_2^{0.873}) \times (1-\alpha)^{2/3}$$

1. Introduction

The Korea Atomic Energy Research Institute (KAERI) is under intensive research on the development of the pyroprocessing, which is an electrochemical reaction technique to recover uranium and transuranic (TRU) nuclides from used nuclear fuel (UNF) in a proliferation-resistant way [1,2]. During the pyroprocessing, three kinds of wastes are generated: 1) filter waste from heat treatment of volatile and semi-volatile nuclides such as I, Cs, Tc, and Ru, 2) electrolyte waste from electro-reduction and electro-refining processes which employ LiCl and LiCl–KCl eutectic salts as the electrolyte, respectively, and 3) metal waste which is composed of hardware, cladding hull and noble metal wastes. Compared to the filter and electrolyte wastes, the metal waste did not bring much attention in the early stage of the pyroprocessing research owing to its relatively low radioactivity and decay heat. But, recent reports showed that the hardware and cladding hull wastes need more investigation owing to their large volume and radioactivity [3,4]. The radioactivation calculation results revealed that these wastes might be categorized into intermediate level waste (ILW) according to the Korean regulation owing to high radioactivity [3]. In addition, these wastes cannot be disposed of in the Wolsung LILW (Low and Intermediate Level Waste) disposal center (WLDS) located in Gyeongju City of Republic of Korea (ROK). In other words, a large amount of ILW will be generated from the pyroprocessing which are not acceptable to the WLDS which is currently the only disposal site of ROK. As about 0.1 MT of hardware and 0.25 MT of cladding hull wastes are generated from the pyroprocessing for every tone of uranium, the amount of metal (and ILW) waste is not negligible at all.

At KAERI, a chlorination process began to be focused owing to its ability to selectively recover zirconium from the cladding hull waste. As zirconium consists of more than 97 wt.% of Zr alloy cladding hulls, a selective recovery of Zr can greatly reduce the amount of ILW from the pyroprocessing. Based on the estimation of KAERI, the amount of ILW generated from the cladding hull waste can be reduced to 1/10–1/20 using the chlorination process. The most significant merits of the chlorination process are 1)

* Corresponding author. Nuclear Fuel Cycle Process Development Division, Korea Atomic Energy Research Institute, Daedeok-daero 989-111, Yuseong-gu, Daejeon 305-353, Republic of Korea.
E-mail address: minku@kaeri.re.kr (M.K. Jeon).

http://dx.doi.org/10.1016/j.jnucmat.2015.05.013
0022-3115/

straightforward reaction between metallic Zr and gaseous chlorine (Eq. (1)) and 2) easy separation of reaction product ($ZrCl_4$) at a low temperature of 331 °C (sublimation temperature of $ZrCl_4$). In other words, we can easily convert metallic zirconium into its chloride form and separate it from the other nuclides including residual UNF and radioactivation products.

$$Zr(s) + 2Cl_2(g) \leftrightarrow ZrCl_4(g) \quad (1)$$

In addition to KAERI, the Oak Ridge National Laboratory (ORNL) of the Unites States is also working on the chlorination process as a part of interim storage of UNF [5]. They performed the chlorination reaction in a hot cell using an actual UNF cladding hull, and reported decontamination factors of 177, 667, and >1200 for ^{241}Am, ^{60}Co, and total radiation, respectively. Institute of Research and Innovation (IRI) of Japan also demonstrated the chlorination process to achieve a successful recovery of zirconium from a mixture of Zircaloy-2 cladding hulls in the presence of CsCl and UO_2 [6]. At KAERI, fundamental approaches including reaction kinetics were mainly made to build a database for scale-up [7–9]. The first approaches were done using a quartz reactor by repeated experiments for various reaction periods [7]. In that study, a linear reaction rate equation was achieved for bare Zircaloy-4 cladding hulls, while delayed reaction rate was observed in oxidized Zircaloy-4 cladding hulls. But precise modeling of the reaction was not possible, because this experiment provided only discrete information. Therefore, development of a thermo-gravimetric analysis (TGA) system for the chlorination reaction of cladding hulls was strongly recommended. Although commercial systems are available which can operate under a chlorine atmosphere, the commercial ones could hold small amount or pieces of cladding hulls. Cladding hulls normally have a diameter close to 1 cm, and intrinsic reaction kinetics of the cladding materials in their powder or other forms might be different from those of tubes owing to heat and mechanical processes applied to manufacture the tubes. Thus, a TGA system which can hold the cladding hulls in its tube form under a chlorine atmosphere was developed at KAERI [8]. But the initial version of the TGA system for the hull chlorination (TGA-HC) exhibited a problem owing to the buoyancy effect. A modified version of the TGA-HC system was successfully demonstrated in our previous work, where the chlorination reaction kinetics of 3 cm long Zircaloy-4 tubes were achieved [9]. Here, it needs to be mentioned that Zircaloy-4 contains Sn, Fe, and Cr as major alloy elements, while ZIRLO has Sn, Nb, and Fe as its alloying constituents. As it was well established that the two cladding materials exhibit significantly different oxidation behaviors [10,11], it is expected that the chlorination reaction mechanism of the two materials can differ. In the present study, the TGA-HC system was employed to investigate the chlorination reaction kinetics of ZIRLO cladding tubes.

2. Experimental

The modified TGA-HC system introduced in our previous work [9] was employed for this study. Briefly, a balance was put on the top of the system which is covered by an acryl box and connected to an argon inlet and computer system through an RS232C cable. As the balance has a hook beneath its bottom, the hook was connected to a quartz sample holder through a stainless steel wire. A quartz reactor of 4 cm diameter was employed as a reactor which covers the sample parts and guides gas flow streams. Chlorine gas was introduced through a port of the quartz reactor to be mixed with argon coming from the top of the system. After the reaction occurs at the heating zone where the sample is held in the middle, the gases (argon and unreacted chlorine) and gaseous reaction products flow downward to reach a cooling zone, where metal chlorides are gathered in their solid form while gases are introduced to a scrubbing system. The weight of the sample was measured for every 10 s by the computer connected to the balance. To verify the chlorination reaction kinetics of ZIRLO cladding hulls, the experiments were performed for various chlorine partial pressures (9.21–23.4 kPa), reaction temperatures (350–600 °C), and total flow rates (120 and 240 mL/min).

3. Results and discussion

3.1. Effect of the gas phase mass transfer

Before establishing reaction equations, it needs to be identified if the reaction is affected by gas phase mass transfer. In a gas–solid reaction, two gas phase phenomena should be considered: gas phase diffusion through the boundary layer and supply of gas phase reactant [12]. The former can be calculated using the Ranz–Marshall equation [13–15]:

$$\frac{dn_{Cl_2}}{dt} = \frac{D_{Ar-Cl_2}\left(2 + 0.6N_{Re}^{\frac{1}{2}}N_{Sc}^{\frac{1}{3}}\right)}{L} \times \frac{(P_{Cl_2,0} - P_{Cl_2,S})}{R_g T} \times A \quad (2)$$

where dn_{Cl_2}/dt is the chlorine molar flow rate, D_{Ar-Cl_2} is the binary diffusion coefficient for Ar-Cl_2 system, N_{Re} is the Reynolds number ($N_{Re} = U \cdot L/\nu$, U is the linear fluid velocity, ν is the kinematic viscosity), N_{Sc} is the Schmidt number ($N_{Sc} = \nu/D_{Ar-Cl_2}$), L is the sample characteristic dimension (diameter of cladding hulls (9.5 mm) was employed), P_{Cl_2} is the chlorine partial pressure at bulk and sample surface (subscript 0 and S, respectively), R_g is the gas constant, T is the absolute temperature, and A is the sample external surface. The Chapman–Enskog theory [12,16] was employed to derive ν and D_{Ar-Cl_2} values. The calculation results under the condition of the present study are listed in Table 1 with experimental values when the conversion fraction is 1/2. The conversion fraction is defined by

$$\alpha = \frac{m_0 - m_t}{m_0 - m_\infty} \quad (3)$$

where m_0 is the initial weight, m_t is the weight at time t, and m_∞ is the weight at the end of the reaction [17]. In this study, m_0 was set to zero before chlorine gas was fed, resulting in negative values for m_t and m_∞ owing to a continuous removal of the reaction products ($ZrCl_4$). One thing should be noted here that the values calculated using the Ranz–Marshall equation assumed that the samples are under a freely flowing gas condition. Thus, it was suggested by Hills [18] and Hakvroot [19] that one order reduction should be applied to the values calculated from the Ranz–Marshall effect for the samples contained in a crucible. As shown in Table 1, the calculated values were about 10 times larger than the measured ones suggesting that the diffusion rate are high enough to be eliminated from a reaction rate equation of this study.

The effect of gas phase supply can be identified by experiments at various total flow rates (Q), because increasing Q might not affect the reaction rate if enough gas phase reactant is supplied already. On the other hand, increasing Q will induce increasing reaction rate in a gas phase deficient condition which is so-called the starvation condition. Fig. 1 shows the experimental results performed at different Q while chlorine partial pressure and temperature were set identical. A significant increase in the reaction rate was observed at 9.21 kPa of pCl_2 with an increase of Q from 120 to 240 mL/min, and an increase of reaction rate was also noticeable at

Table 1
List of calculated and measured chlorine molar flow rates.

T (°C)	Total flow rate (mL/min)	Chlorine partial pressure (kPa)	dn_{Cl_2}/dt [calculated] (mol/s)	dn_{Cl_2}/dt [measured, $\alpha = 0.5$] (mol/s)
400	120	9.21	3.608×10^{-5}	1.864×10^{-6}
400	120	16.9	6.620×10^{-5}	2.713×10^{-6}
400	120	23.4	9.166×10^{-5}	4.656×10^{-6}
350	120	16.9	6.327×10^{-5}	2.425×10^{-6}
500	120	16.9	7.210×10^{-5}	5.146×10^{-6}
600	120	16.9	7.765×10^{-5}	8.183×10^{-6}

16.9 kPa of pCl_2 when Q increased from 120 to 180 mL/min. This result suggests that the conditions of these experiments are under the influence of total flow rate, in other words, the experiments were performed in the starvation condition. In the present study, the total flow rate was fixed at 120 mL/min owing to limitations of the TGA system, and to compare the results with those of Zircaloy-4 shown in our previous work [9]. Thus, the Q term was not considered as a variable in the present study, but it should be noted that the reaction rate might increase with increasing Q.

3.2. Determination of geometry function

In a solid–gas reaction, a morphological change of solid phase should be included in reaction rate equations. Thus, determining a suitable geometry function is a key step in completing a reaction rate equation. The geometry function is normally divided into four categories of nucleation (and growth), geometrical contraction, diffusion, and reaction-order models [17]. One can determine the most suitable model 1) by comparing ($d\alpha/dt$) versus α graphs because each model has characteristic shape, 2) by fitting experimental results for all models, or 3) by using the Sharp–Hancock plot [20]. The third option was employed in the present study, because it was identified in our previous work on Zircaloy-4 that a change of reaction mechanism occurs during the reaction [9], and the Sharp–Hancock plot can clarify simultaneously both the most suitable reaction mechanism and a region where the mechanism is

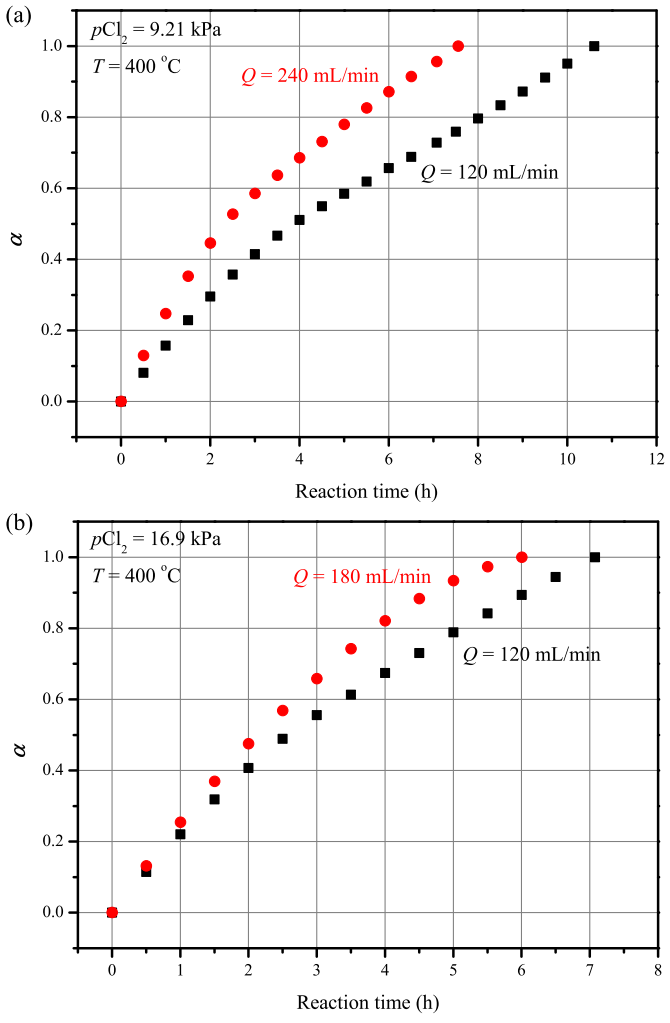

Fig. 1. Influence of total flow rate on the chlorination reaction rate of ZIRLO when chlorine partial pressure is (a) 9.21 and (b) 16.9 kPa.

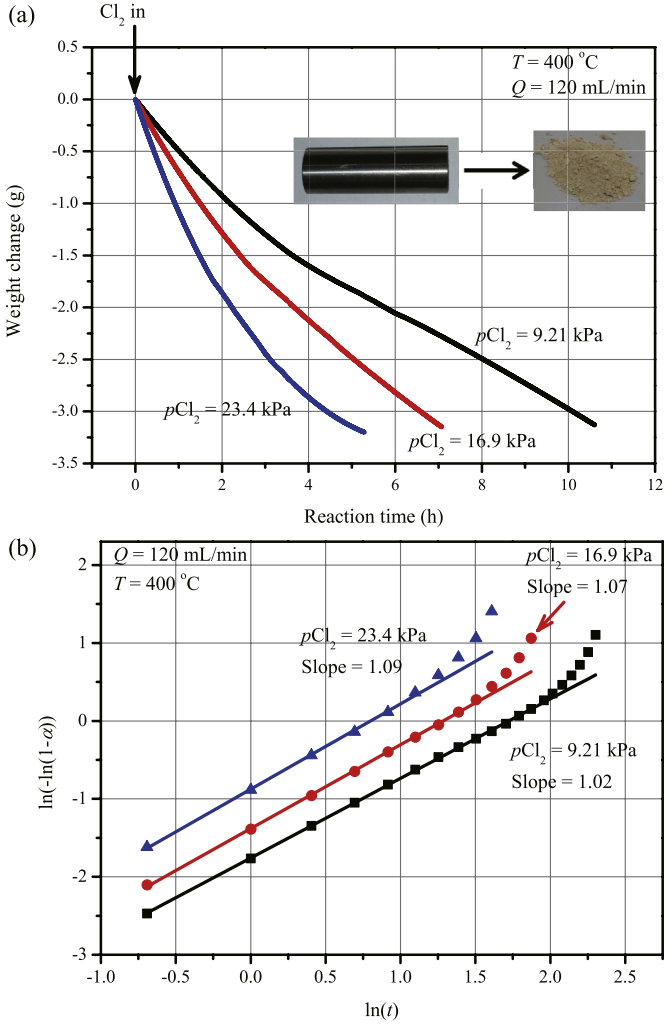

Fig. 2. (a) The experimental results and (b) their Sharp–Hancock plot fitting results as a function of chlorine partial pressure at T = 400 °C and Q = 120 mL/min condition. Insets of (a) are pictures of bare ZIRLO cladding hull and recovered $ZrCl_4$.

available. The Sharp–Hancock plot can be achieved using an equation of

$$\ln[-\ln(1-\alpha)] = \ln(B) + m\ \ln(t) \tag{4}$$

where B is a constant and m is a slope of $\ln[-\ln(1-\alpha)]$ versus $\ln(t)$ plot. A linear region of the Sharp–Hancock plot indicates that this region shares an identical reaction mechanism, and the slope (m) of the linear region reveals which geometry function is the most suitable [12]. The experimental results performed as a function of chlorine partial pressure and their Sharp–Hancock plot fitting results are shown in Fig. 2. The Sharp–Hancock plots revealed that linear fitting was available for different regions ($0 \le \alpha \le 0.69$ at $pCl_2 = 9.21$ kPa, $0 \le \alpha \le 0.73$ at $pCl_2 = 16.9$ kPa, and $0 \le \alpha \le 0.50$ at $pCl_2 = 23.4$ kPa). It is worth mentioning that the linear region is relatively narrow in the 23.4 kPa case although the reason cannot be accounted for at this stage. To achieve a reaction equation which can cover the range of chlorine partial pressure, the range where the geometry function is available was limited to $0 \le \alpha \le 0.50$ through this work. As noted above, the slope of the linear fitting results can reveal the most suitable geometry function. An average slope value of 1.06 was achieved from Fig. 2, which means that a contracting volume model (slope = 1.07) is the most suitable one as the case of Zircaloy-4 [9]. The contracting volume model is expressed as:

$$g(\alpha) = 1 - (1-\alpha)^{1/3} = k_{app}t \tag{5}$$

where k_{app} is the apparent reaction constant and t is reaction time (h).

3.3. Effect of chlorine partial pressure

The reaction rate of a solid–state reaction can be written as:

$$R = \frac{d\alpha}{dt} = k(T)F(pCl_2)G(\alpha) \tag{6}$$

where $k(T)$ accounts for the effect of reaction temperature, $F(pCl_2)$ represents the effect of chlorine partial pressure, and $G(\alpha)$ is a differentiation form of $g(\alpha)$. Combining Eqs. (5) and (6), a following equation is derived:

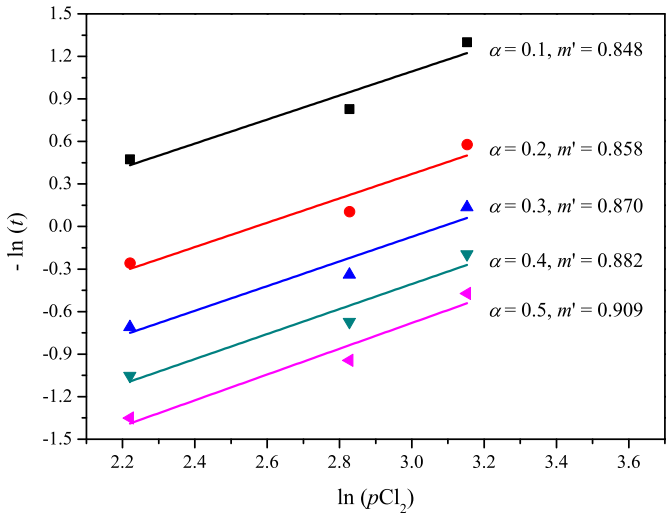

Fig. 3. The $-\ln(t)$ versus $\ln(pCl_2)$ fitting results at $T = 400$ °C and $Q = 120$ mL/min condition.

$$g(\alpha) = 1 - (1-\alpha)^{1/3} = k_{app}t = k(T) \times f(pCl_2) \times t \tag{7}$$

where $k(T)$ is an Arrhenius equation and $f(pCl_2)$ is an integral form of $F(pCl_2)$. Eq. (7) can be expressed as following by assuming that $f(pCl_2)$ employs a power law type dependence on chlorine partial pressure:

$$g(\alpha) = 1 - (1-\alpha)^{1/3} = k_{app}t = k(T) \times A' \cdot pCl_2^{m'} \times t \tag{8}$$

where A' is a constant and m' is reaction order. Eq. (8) can be rearranged as:

$$\frac{1}{t} = \frac{k(T)\cdot A' \cdot Q'}{1-(1-\alpha)^{1/3}} \times (pCl_2)^{m'} \tag{9}$$

$$-\ln(t) = \ln\left[\frac{k(T)\cdot A' \cdot Q'}{1-(1-\alpha)^{\frac{1}{3}}}\right] + m' \times \ln(pCl_2) \tag{10}$$

Eq. (10) reveals that the m' value can be achieved from a slope of $-\ln(t)$ versus $\ln(pCl_2)$ graph, and the fitting results are illustrated in Fig. 3. The m' value was identified as 0.873 from an average of the five α cases.

3.4. Effect of reaction temperature

By using the Arrhenius equation and m' value of 0.873, Eq. (8) can be re-written as follows:

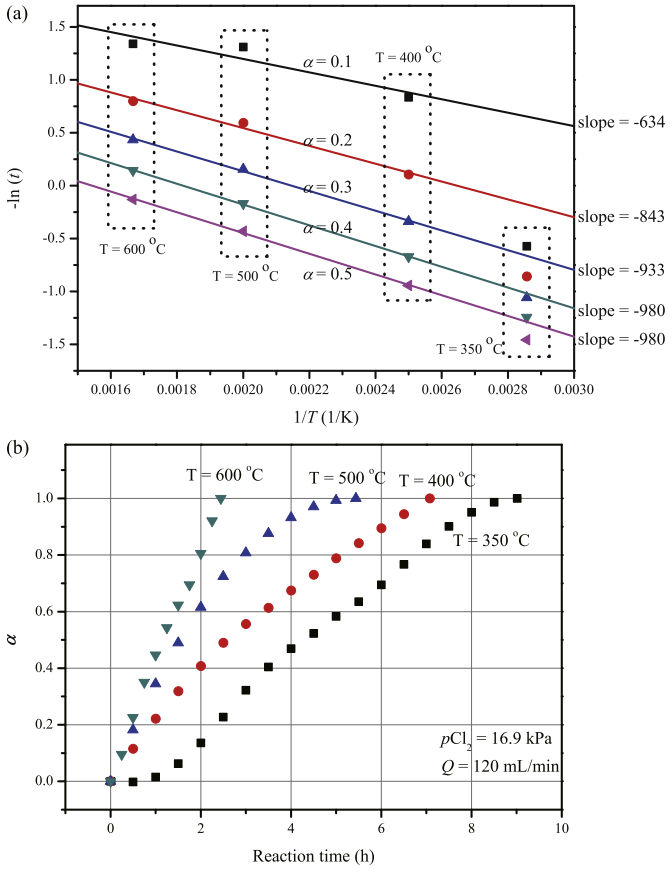

Fig. 4. (a) The $-\ln(t)$ versus $1/T$ graph and fitting results for various reaction temperatures and α values. (b) Experimental results obtained for various reaction temperatures at $pCl_2 = 16.9$ kPa and $Q = 120$ mL/min condition.

$$g(\alpha) = 1-(1-\alpha)^{\frac{1}{3}} = k(T)\times A'\cdot pCl_2^{0.873}\times t = k_0\cdot e^{-\frac{E_a}{R_g T}}\times pCl_2^{0.873}\times t \quad (11)$$

where k_0 is an apparent pre-exponential factor which includes A', E_a is an activation energy, and R_g is the gas constant. For experiments performed at identical pCl_2 condition, the pCl_2 term can be regarded as a constant resulting in following equations:

$$\frac{1}{t} = \frac{k_0\cdot pCl_2^{0.873}}{1-(1-\alpha)^{1/3}}\times e^{-\frac{E_a}{R_g T}} \quad (12)$$

$$-\ln(t) = \ln\left[\frac{k_0\cdot pCl_2^{0.873}}{1-(1-\alpha)^{\frac{1}{3}}}\right] + \left(-\frac{E_a}{R_g}\right)\frac{1}{T} \quad (13)$$

The fitting results obtained using Eq. (13) are shown in Fig. 4(a) for the temperature range of 350–600 °C. But, it was identified that the results of 350 °C were not in line with the results of other temperatures suggesting that the reaction is under the influence of other parameters at this temperature. As shown in Fig. 4(b), an incubation time was observed for the results of 350 °C experiment, which accounts for the fitting results of Fig. 4(a). Back to Fig. 4(a), slopes of the graphs were calculated resulting in −874 as an average leading to an activation energy of 7.27 kJ/mol. This value is significantly lower than 26.2 kJ/mol of the Zircaloy-4 case [9], and it can be interpreted as high reaction rate and gas phase transport limited reaction. Because it is normally accepted that low activation energy below 25 kJ/mol indicates gas phase transport limited reaction, and it was already discussed in Fig. 1. In addition, calculation of the k_0 values for increasing reaction temperature from 400 to 500, and 600 °C resulted in an increase of the k_0 values from 0.02477 to 0.03482, and 0.04004, respectively. These results lead to a conclusion that both Arrhenius equation term and gas phase transport affects the reaction rate, and the effect of each term cannot be clarified in this study owing to a mechanical limitation in increasing total flow rate. Thus, the final form of Eq. (11) should have a limited version as follows:

$$g(\alpha) = 1-(1-\alpha)^{\frac{1}{3}} = 0.00738\times pCl_2^{0.873}\times t \quad (14)$$

The value (0.00738) was achieved from an average value of fitting results for various pCl_2. Here, in addition, it needs to be declared that Eq. (14) is valid only when Q = 120 mL/min and T = 400 °C condition. From Eq. (14), final forms of reaction rate equations can be derived as following, and the final fitting results are shown in Fig. 5:

$$\alpha = 1-\left(1-0.00738\times pCl_2^{0.873}\times t\right)^3 \quad (15)$$

$$\frac{d\alpha}{dt} = 3\times\left(0.00738\times pCl_2^{0.873}\right)\times(1-\alpha)^{2/3} \quad (16)$$

Here, it might be helpful to discuss what should be done to achieve more precise reaction rate equation that includes the effects of reaction temperature and excludes the gas phase transport limitation. Currently, the maximum flow rate for argon and chlorine gases are 300 and 30 mL/min, respectively, and it is hard to increase the flow rate because it has quartz and pyrex parts connected with 24/40 joints. Thus, the reactor design should be modified so that it can handle higher flow rate to eliminate the gas phase transport effects. The effect of temperature part might be clarified under a high flow rate condition, and heating up to higher temperature will be helpful. But, validity of a new system might be

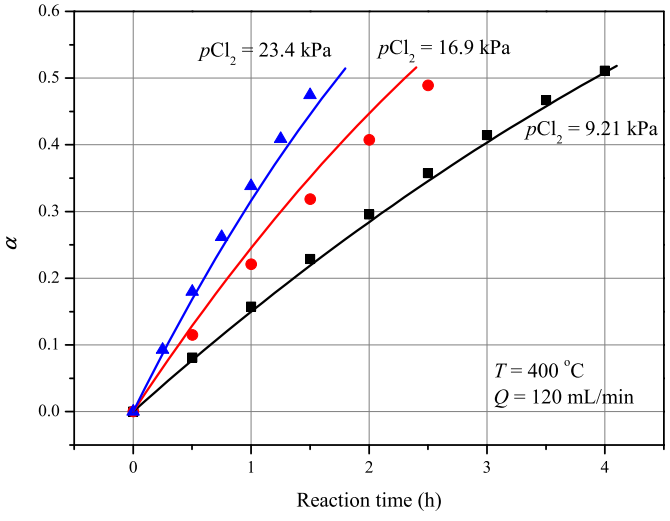

Fig. 5. The experimental and final fitting results achieved using Eq. (15) as a function of chlorine partial pressure at T = 400 °C and Q = 120 mL/min.

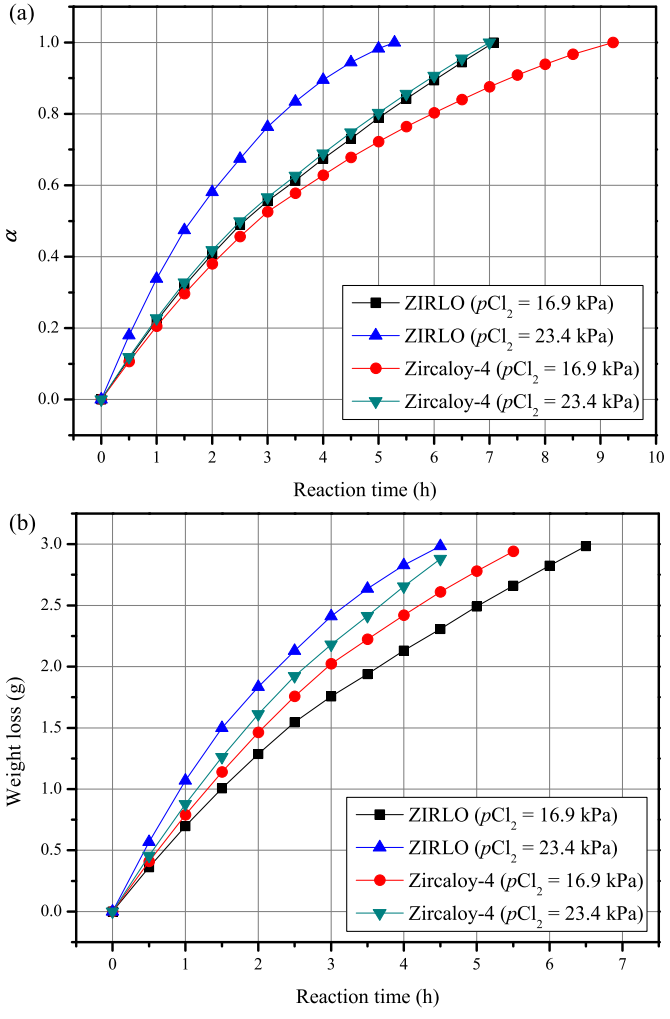

Fig. 6. Chlorination reaction experiment results for ZIRLO and Zircaloy-4 at 400 °C and Q = 120 mL/min condition. (a) Experimental results for 3 cm long pieces and (b) redrawing of (a) considering weight of each cladding hull.

required before the high temperature experiments, because higher temperature brings larger buoyancy force to the sample.

3.5. ZIRLO versus Zircaloy-4

It would be interesting to compare the chlorination reaction behavior between ZIRLO and Zircaloy-4 cladding materials. As noted in the introduction section, these two alloys have different major alloying metals; ZIRLO contains Nb, Sn, and Fe, while Zircaloy-4 includes Sn, Fe, and Cr. In Fig. 6(a), a comparison was made for the chlorination reaction behavior between the two alloys when an identical length (3.0 cm) and experimental condition were employed. In the $0 \leq \alpha \leq 0.5$ region where the volumetric contraction model is applicable, the difference is not significant when chlorine partial pressure is 16.9 kPa, while significant increase in the reaction rate was observed in the ZIRLO case when the chlorine partial pressure increased to 23.4 kPa. This result came from the different influence of chlorine partial pressure on the reaction rate; for ZIRLO reaction rate was proportional to ($pCl_2^{0.873}$) while it was ($pCl_2^{0.669}$) for Zircaloy-4 (Eq. 19 of Ref. 9). Considering that ZIRLO and Zircaloy-4 have different weight for 3 cm long pieces (3.16 g for ZIRLO and 3.85 g for Zircaloy-4), Fig. 6(a) was redrawn based on weight loss in Fig. 6(b). When pCl_2 is 16.9 kPa, the reaction rate of ZIRLO is slower than that of Zircaloy-4, while that of ZIRLO is significantly increased when pCl_2 increased to 23.4 kPa. This result suggests that increasing pCl_2 can accelerate the reaction rate for both cases, but the effect will be more significant in ZIRLO as shown in Fig. 6.

Significant differences between ZIRLO was Zircaloy-4 were also revealed in the total flow rate and reaction temperature experiments. It was identified that, under the condition of this work, ZIRLO is under the gas phase transport limitation region, while Zircaloy-4 is not. This result means that increasing total flow rate will cause an increase in the reaction rate of ZIRLO while no changes will be made for Zircaloy-4. The activation energy values achieved from the experiments were 7.27 and 26.2 kJ/mol for ZIRLO and Zircaloy-4, respectively, meaning that increasing reaction temperature will contribute to an increase of reaction rate more significantly in ZIRLO, although the value for ZIRLO is not certain. It also needs to be recognized that the ZIRLO cladding hulls were not reactive at 300 °C, while Zircaloy-4 hull were. In summary, it can be concluded that the chlorination reaction rate of Zircaloy-4 is superior at low temperature, low pCl_2, and low total flow rate, but increasing T, pCl_2, and Q will increase the reaction rate of ZIRLO more significantly.

Using the TGA-HC system, the chlorination reaction rates of Zircaloy-4 and ZIRLO were achieved although the system needs further modifications for ZIRLO application as discussed above. For the final purpose of this work, fabrication of a commercial-scale cladding hull waste chlorination system, the TGA-HC system might need further research to simulate the behavior of actual cladding hulls. First of all, the next work should be done for oxidized cladding hulls, because actual cladding hulls have micrometers thick oxide layers on their side walls. It was qualitatively identified that oxidized cladding hulls suffer from incubation time [5] or late reaction rate in an early stage of the chlorination reaction [7]. A quantitative analysis on the effect of oxide layer formation can be identified using the TGA-HC system, and the results will contribute to the design of a large scale cladding hull chlorination system. The effect of cross-section opening is also an interesting issue. Actual cladding hulls might have bare or slightly oxidized cross-sections generated during shearing or cutting processes. These processes are normally performed before the chlorination process to separate nuclear materials from cladding hulls. The exposure of fresh cross-sections might help to initiate and accelerate the chlorination reaction, although quantitative contribution needs to be identified. One more issue not to be missed is purification of recovered $ZrCl_4$. As chlorides of some alloying constituents including Sn, Nb, and Fe will be evaporated and recovered with $ZrCl_4$, purification of $ZrCl_4$ might be necessary for disposal or re-use. The TGA-HC system can be a powerful tool for the $ZrCl_4$ purification study as it contains the recovery part in its bottom.

4. Conclusion

The chlorination reaction rate for ZIRLO cladding hulls was studied using the TGA-HC system resulting in a following equation:

$$\frac{d\alpha}{dt} = 3 \times \left(0.00738 \times pCl_2^{0.873}\right) \times (1-\alpha)^{2/3}$$

The effect of reaction temperature could not be identified, because the reaction condition of the present study lied within the gas phase transport limited region. Thus, the reaction equation achieved in the present study is valid only at 400 °C of reaction temperature and 120 mL/min of total flow rate. Modification of the TGA-HC system to handle higher flow rate is necessary to achieve more precise reaction rate equation for the chlorination reaction of ZIRLO. Issues to be managed using the TGA-HC system in the future for the fabrication of a commercial-scale cladding hull waste chlorination reactor could be summarized as follows: 1) the effect of oxide layers on the chlorination reaction rate, 2) the effect of cross-section opening on the reaction rate, and 3) purification of recovered $ZrCl_4$.

Acknowledgment

This work was sponsored by the Nuclear R&D program of the Korean Ministry of Science, ICT & Future Planning (No. 2012M2A8A5025697).

References

[1] H. Lee, G.I. Park, K.H. Kang, J.M. Hur, J.G. Kim, D.H. Ahn, Y.Z. Cho, E.H. Kim, Nucl. Eng. Technol. 43 (2011) 317–328.
[2] K.C. Song, H. Lee, J.M. Hur, J.G. Kim, D.H. Ahn, Y.Z. Cho, Nucl. Eng. Technol. 42 (2010) 131–144.
[3] M.K. Jeon, C.H. Lee, C.J. Park, J.H. Choi, I.H. Cho, K.H. Kang, H.S. Park, G.I. Park, J. Radioanal. Nucl. Chem. 298 (2013) 1629–1633.
[4] M.K. Jeon, C.J. Park, C.H. Lee, K.H. Kang, G.I. Park, J. Radioanal. Nucl. Chem. 292 (2012) 1221–1228.
[5] E.D. Collins, G.D. Del Cul, B.B. Spencer, R.R. Brunson, J.A. Johnson, D.S. Terekhov, N.V. Emmanuel, Proc. Chem. 7 (2012) 72–76.
[6] Y. Yasuike, S. Iwasa, K. Suzuki, H. Kobayashi, O. Amano, N. Sato, in: Proceedings of ICEM'03: The 9th International Conference on Radioactive Waste Management and Environmental Remediation, Oxford, England, 2003.
[7] M.K. Jeon, C.H. Lee, C.M. Heo, Y.L. Lee, Y.T. Choi, K.H. Kang, G.I. Park, J. Korean Radioact. Waste Soc. 11 (2013) 69–75.
[8] M.K. Jeon, Y.T. Choi, C.H. Lee, Y.L. Lee, K.H. Kang, G.I. Park, Trans. Am. Nucl. Soc. 108 (2013) 163–164.
[9] M.K. Jeon, Y.T. Choi, K.H. Kang, G.I. Park, J. Nucl. Mater. 459 (2015) 175–182.
[10] M. Steinbrück, N. Vér, M. Große, Oxid. Met. 76 (2011) 215–232.
[11] H.H. Kim, J.H. Kim, J.Y. Moon, H.S. Lee, J.J. Kim, Y.S. Chai, J. Mater. Sci. Technol. 26 (2010) 827–832.
[12] J. Szekely, J.W. Evans, H.Y. Sohn, Gas-Solid Reactions, Academic Press, USA, New York, 1976.
[13] W.E. Ranz, W.R. Marshall Jr., Chem. Eng. Prog. 48 (1952) 141–146.
[14] W.E. Ranz, W.R. Marshall Jr., Chem. Eng. Prog. 48 (1952) 173–180.
[15] J.P. Garviría, G.G. Fouga, A.E. Bohé, Thermochim. Acta 517 (2011) 24–33.
[16] G.H. Geiger, D.R. Poirier, Transport Phenomena in Metallurgy, Addison-Wesley, Massachusetts, MA, 1973.
[17] A. Khawam, D.R. Flanagan, J. Phys. Chem. B 110 (2006) 17315–17328.
[18] A.W.D. Hills, Metall. Trans. B 9 (1978) 121–128.
[19] G. Hakvoort, Thermochim. Acta 233 (1994) 63–73.
[20] J.D. Hancock, J.H. Sharp, J. Am. Ceram. Soc. 55 (1972) 74–77.